ACS APPLIED MATERIALS & INTERFACES

Research Article

www.acsami.org

Synthesis of an Fe Rich Amorphous Structure with a Catalytic Effect To Rapidly Decolorize Azo Dye at Room Temperature

Peng Liu,*[,†] Ji Liang Zhang,[†] Mei Qin Zha,[‡] and Chan Hung Shek*[,†]

[†]Department of Physics and Materials Science, City University of Hong Kong, Kowloon Tong, Hong Kong, China

[‡]Department of Biology and Chemistry, City University of Hong Kong, Kowloon Tong, Hong Kong, China

Supporting Information

ABSTRACT: In this article, an amorphous Fe rich amorphous structure designed based on a competitive atomic cluster model was synthesized and characterized successfully. The constituent zero-valent iron (ZVI) has excellent activity and efficiency for decolorization of Orange G (OG) solution at room temperature. The decolorization is characterized by UV-vis spectrum and pseudo-first-order kinetics. The X-ray Micro fluorescence spectrometer, Inductively Coupled Plasma Optical Emission Spectrometry, and Scanning Electron Microscope were employed to trace the ZVI. The consumption of ZVI destabilizes the local atomic arrangement and yields the phase separation of Fe at the surface and responds to the high activity and the catalysis for decolorization. This observation is in accordance with the change of k_1 0.011 min^{-1} to k_2 0.047 min^{-1}, which is supported by the cyclic decolorization test. This work provides a new strategy to design multifunctional metal materials and indicates their brilliant future in practical applications.

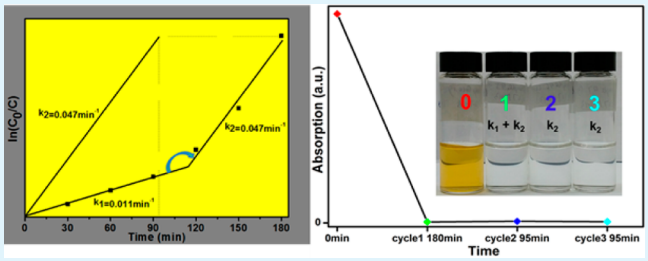

KEYWORDS: *amorphous structure, competitive atomic arrangement, zero-valent iron, rapid decolorization, catalysis*

INTRODUCTION

The ZVI is prevalent in water remediation since it was proved to be an efficient reductant to decompose plentiful chemical hazard such as Nitro aromatic compounds,[1] Halogenated organic compounds,[2] and Azo dyes.[3,4] The advantage of ZVI lies at its abundance and nontoxicity. However, it requires very stringent conditions to keep its high activity and is easy to oxidize or to form hydroxide over the surface.[3,5] Recent studies indicate that the amorphous ZVI powder has lower activation energy and thus higher activity than its crystalline counterparts.[6,7] However, in an amorphous structure, the atomic environment of ZVI can vary significantly, which implies large differences in stability, and properties may exist in the system even with similar compositions.[8] Herein, we report a new ZVI in the form of glassy $Fe_{66.3}B_{16.6}Y_{17.1}$ structure designed on the principle of competitive atomic clusters.

The popular opinions[9,10] agree that amorphous solid fabricated from rapid quenching of liquids contains generally close-packed clusters as the primary units, bridged by glue atoms or clusters. The bonding between glue atoms/clusters and the primary units is vulnerable compared with the bonding in primary units. Thus, these weak bondings are more sensitive and readily detached. Obviously, ZVI at these sites will be more ready for the function. In this case, the content of Fe is not the only factor as the iron could be anchored either in primary units or glue atoms/clusters. Inspired by the idea, we introduce a comparable fraction of another Fe-rich cluster to compete with the well-known Fe_8B_2 cluster.[11,12] The interaction between two comparable primary clusters is expected to destabilize each other and yield weak bonding in these clusters.

The free energy of the system can also rise as a result of the competition of these clusters and higher entropy. It has been reported that Yttrium can effectively facilitate the fabrication of Fe-rich amorphous structures, so we decided to choose another cluster in the Fe−Y system.[13] According to the Fe−Y phase diagram,[14] there are three eutectic reactions on the Fe-rich side. The eutectic points at 12.9 at% and 23.7 at% show relatively low melting temperatures, and a compound $Fe_{23}Y_6$ locates between the two eutectic compositions. Thus, we extracted the $Fe_{11}Y_3$ as a eutectic cluster from the $Fe_{23}Y_6$ compound. The Fe_8B_2 and $Fe_{11}Y_3$ clusters are selected to develop a novel amorphous structure, in which the competitions between clusters weaken the bonds per atom and thus destabilize the atomic structure.[15] It can be approached using a cluster line model,[9] and the composition $Fe_{66.3}B_{16.6}Y_{17.1}$ is located exactly at the intersection of straight composition lines $Fe_{11}Y_3$−B and Fe_8B_2−Y as illustrated in Figure 1. The two composition lines are defined as cluster lines, which extend from binary clusters $Fe_{11}Y_3$ and Fe_8B_2 and point to their respective third elements.

The ZVI in an amorphous structure was successfully fabricated in a foil form and used to rapidly decolorize OG with the efficiency of 99.7%. The OG is a common model selected from Azo dyes that exist in huge amounts in industrial

Received: December 6, 2013
Accepted: March 26, 2014
Published: March 26, 2014

   dx.doi.org/10.1021/am501014s | ACS Appl. Mater. Interfaces 2014, 6, 5500−5505

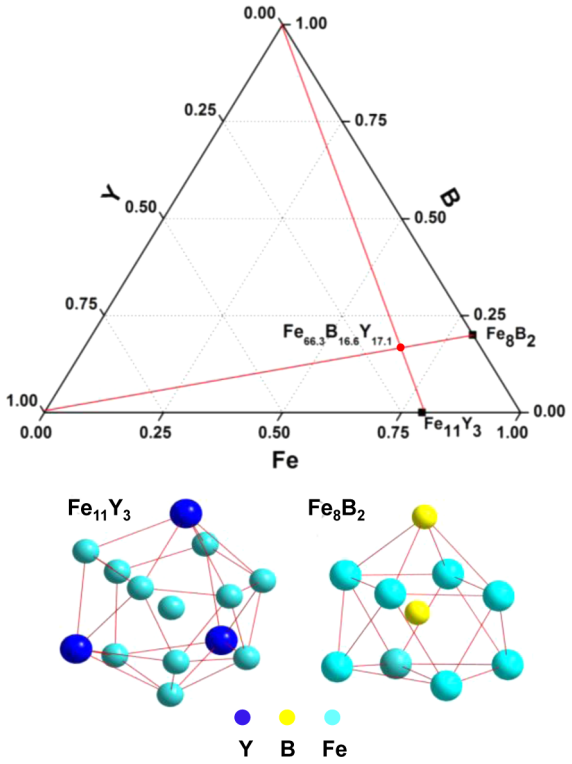

Figure 1. Composition chart of $Fe_{66.3}$ $B_{16.6}Y_{17.1}$ ternary system and cluster lines.

wastewater and present a hazard to nature.[16−18] The destabilized structure of $Fe_{66.3}B_{16.6}Y_{17.1}$ designed on the principle of competitive atomic clusters gives the ZVI a ten times higher reaction rate than that in the Fe−Si−B system[6,7] at room temperature (20° ± 2C). It also provides a new strategy to provide high activity ZVI that is held in an amorphous structure.

EXPERIMENTAL SECTION

All raw metals were commercially available with purity higher than 99.9% and were remelted to minimize the oxygen. The master ingot of $Fe_{66.3}B_{16.6}$ $Y_{17.1}$ was made by arc-melting the Y and Fe−B alloy in ultra-vacuum under a Ti-gettered Argon atmosphere. The ingot of $Fe_{11}Y_3$ was also made through the same way. The foils were produced by a single roller melt-spinning apparatus and cut to approximately 2 mm × 15 mm pieces before use. The $Fe_{79}B_{15}Si_5$ foil in which the Fe_8B_2 existed as a primary unit[19] was purchased from Good Fellow (UK) and used directly. Pure iron powder and analytical grade Orange G ($C_{16}H_{10}N_2Na_2O_7S_2$, MW = 452.37g/mol) were purchased from ALDRICH and used directly.

Typically, the decolorization process was undertaken at room temperature (20° ± 2C). The foil dosage was set at a ratio 0.47 g/35 mL (foil/OG), and the OG aqueous solution was prepared as 100 mg/L with pH = 6. The mixed reactant was held in a sealed glass bottle under continuous stirring. About 1.0 mL of filtrate was taken out at 30 min intervals and diluted to meet the calibration curve.

Phase identification was conducted by X-ray Diffraction (XRD, Philips X'pert X-ray diffracto meter) with Cu−Kα radiation (0.15406 nm). X-ray photoelectron spectroscopy (XPS, ULVAC-PHI 5802 system) with monochromatized Al Kα radiation (1486.6 eV) was employed to characterize the valence band structure of the ZVI in various forms. A UV-vis spectrometer (Perkin Elmer, Lambade2S) was used to collect absorption spectrum of the filtrates and the Inductively Coupled Plasma Optical Emission Spectrometry (ICP-OES, PerkinElmer Optima 2100 DV) was employed to identify the elements leached out into solution. A Scanning Electron Microscope (SEM with EDX, model No. JEOL JSM 820, JEOL Ltd.) was used for examining the surface morphologies of the foils after immersion in OG solution. An X-ray Micro fluorescence spectrometer (XRMF, EDAX Eagle III) with a 40 W X-ray tube (Mo) and a 1 mm spot aperture was used to verify the metals in the sediments. Magnetic measurements were carried out on a vibrating sample magnetometer (Cryogenic, UK) with a maximum field up to 50 kOe.

The rate of decolorization is defined as

$$\text{Decolorization rate} = \frac{C}{C_0} \tag{1}$$

The kinetic of decolorization is expressed as

$$\ln \frac{C_0}{C} = k_{obs}t \tag{2}$$

Half-life time:

$$t_{1/2} = \frac{\ln 2}{k_{obs}} \tag{3}$$

C_0 is the initial OG concentration, C is the OG concentration at time t, k_{obs} is the observed pseudo-first-order decolorization rate constant, and t is the elapsed time of reaction.

$$\text{Decolorization efficiency} = \frac{100(A_0 - A)}{A_0}\% \tag{4}$$

A_0 is the initial absorption, and A is the absorption at time t.

RESULTS

Characterization of Foils. As shown in Figure 2, the $Fe_{79}B_{16}Si_5$ exhibits a diffuse halo peak at 2θ of 45° corresponding to the amorphous nature, while the halo peak at 42° is observed in $Fe_{66.3}B_{16.6}Y_{17.1}$ and $Fe_{11}Y_3$.

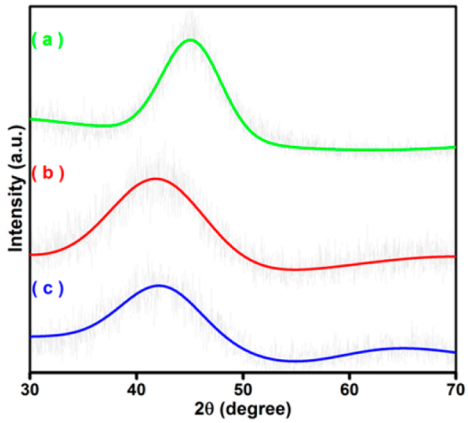

Figure 2. The XRD patterns of $Fe_{79}B_{16}Si_5$ (a), $Fe_{66.3}B_{16.6}Y_{17.1}$ (b), and $Fe_{11}Y_3$ (c).

According to Figure 3, both samples show high density of states that belong to Fe-3d in the vicinity of the Fermi level (E_F). The spectrum of $Fe_{79}B_{16}Si_5$ has a hump centered at 8.7 eV, which resulted from the strong hybridization between Fe-3d and B-2p electrons.[20,21] In the $Fe_{66.3}B_{16.6}Y_{17.1}$, the peak is shifted to 10.6 eV, which was close to the peak of the B-2p band.[22] The profile of the Fe-3d peak has a shoulder at 2.5−3.5 eV, which was similar to pure iron[23] but obviously different from the single sharp peak of $Fe_{79}Y_{21}$[24] that has composition similar to $Fe_{11}Y_3$.

OG Decolorization. OG is a water-soluable salt and dissolves easily in water at room temperature. The fresh color of the OG solution originates from the characteristic absorption

dx.doi.org/10.1021/am501014s | ACS Appl. Mater. Interfaces 2014, 6, 5500−5505

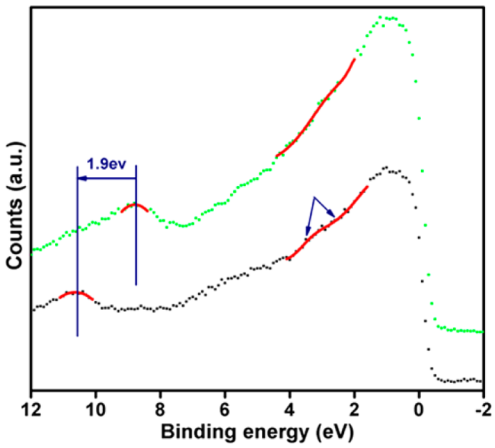

Figure 3. Valence band XPS spectrum of $Fe_{79}B_{16}Si_5$ (green) and $Fe_{66.3}B_{16.6}Y_{17.1}$ (black).

of the "-N═N-" bond at 478 nm. The color gradually decayed with decolorization time after addition of the ZVI foils. The recorded absorptions at 478 nm at 30 min intervals are used to plot the decolorization rate (Figure 4). The results indicated

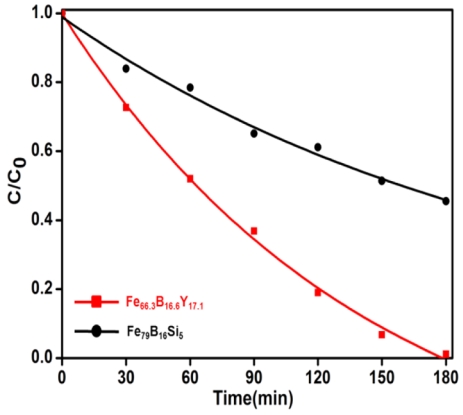

Figure 4. The decolorization of OG over various amorphous ZVI.

that the decolorization could be fully done in 180 min with $Fe_{66.3}B_{16.6}Y_{17.1}$ but not with the $Fe_{79}B_{16}Si_5$. The same data were also used to plot the observed k by pseudo-first-order dynamics.[25] The results of $Fe_{66.3}B_{16.6}Y_{17.1}$ showed a two-stages kinetics with k_1 = 0.011 min^{-1} and k_2 = 0.047 min^{-1} (Figure 5a), while the k of $Fe_{79}B_{16}Si_5$ was 0.0044 min^{-1} (Figure 5b).

Decolorization of OG with the iron powder and $Fe_{11}Y_3$ were also done for a fixed duration (Figure 6). The untreated OG

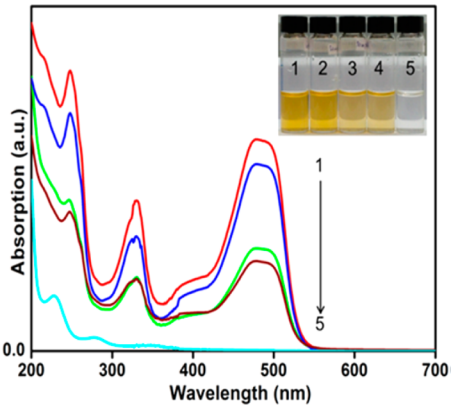

Figure 6. UV-vis spectrum after 180 min decolorization: initial OG (1), iron powder (2), $Fe_{79}B_{16}Si_5$ (3), $Fe_{11}Y_3$ (4), $Fe_{66.3}B_{16.6}Y_{17.1}$ (5).

solution has three peaks at 248, 330, and 480 nm and a shoulder from 370 to 420 nm. The peaks at 248 and 330 nm were caused by aromatic rings, while the peak at 480 nm and the shoulder at 370−420 nm were generated by an azo-bond and its conjugated structure.[18] After 180 min, three of the treated solutions still had the absorption peak at 478 nm except the colorless one, which was decolorized by $Fe_{66.3}B_{16.6}Y_{17.1}$. The colorless solution also had two absorption peaks at 228 and 280 nm, corresponding to aniline.[26]

SEM observations showed the morphology of the foils after immersing in the OG solution for 180 min. The $Fe_{79}B_{16}Si_5$ has only several long and narrow slits (Figure S1a), whereas the $Fe_{11}Y_3$ exhibits some cracks on the protrusion of the surface (Figure S1b). However, the $Fe_{66.3}B_{16.6}Y_{17.1}$ has a porous surface like a beehive (Figure S1c), which indicates that it had experienced an intensive reaction. The holes had a diameter of approximately 10 μm, and one of them (Figure 7a and 7b) was selected for compositional mapping. As shown in Figure 7c and 7d, the center of the hole was enriched with Fe, while the area along its edge had a high Y content.

The room temperature magnetization curve (Figure S2) indicates the soft magnetic property of $Fe_{66.3}B_{16.6}Y_{17.1}$, which

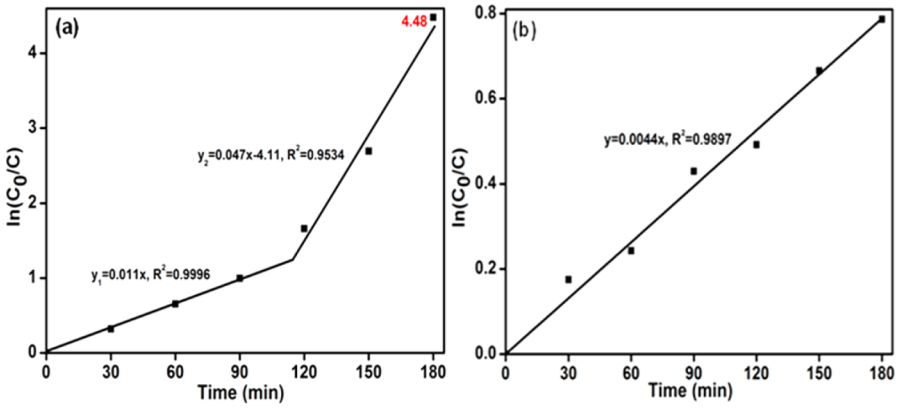

Figure 5. Plotted k of $Fe_{66.3}B_{16.6}Y_{17.1}$ (a) and $Fe_{79}B_{16}$ Si_5 (b).

dx.doi.org/10.1021/am501014s | ACS Appl. Mater. Interfaces 2014, 6, 5500−5505

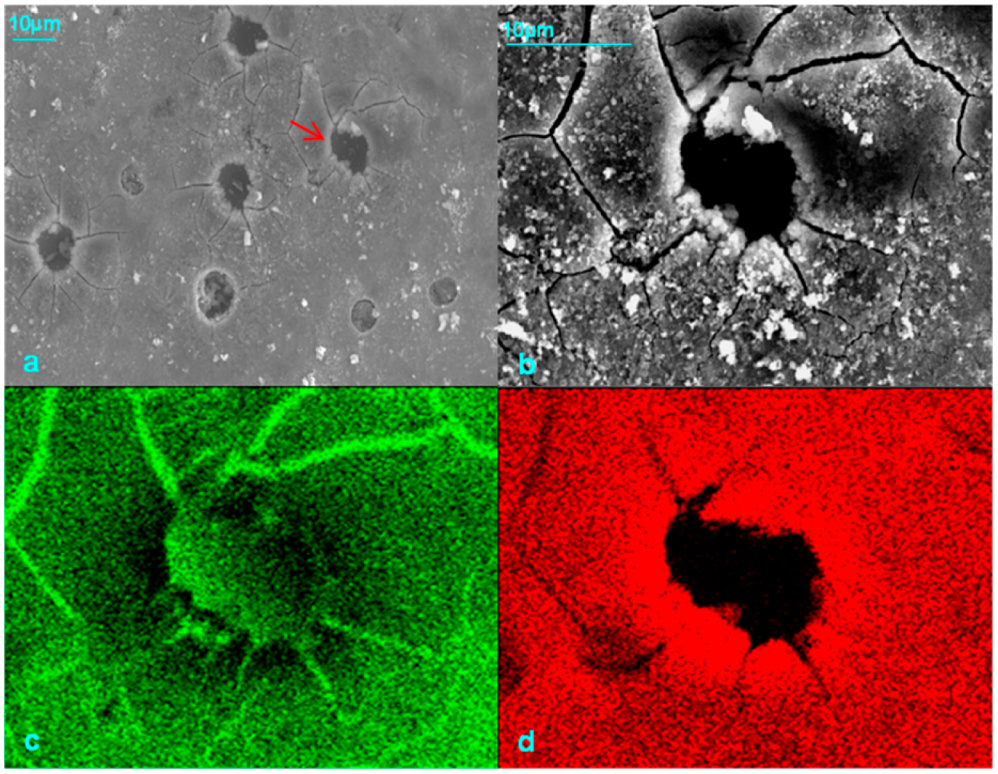

Figure 7. SEM photos of $Fe_{66.3}B_{16.6}Y_{17.1}$ (a, b, c: Fe mapping, d: Y mapping) after 180 min.

Scheme 1. Proposed Decolorization Mechanism of OG by Amorphous ZVI

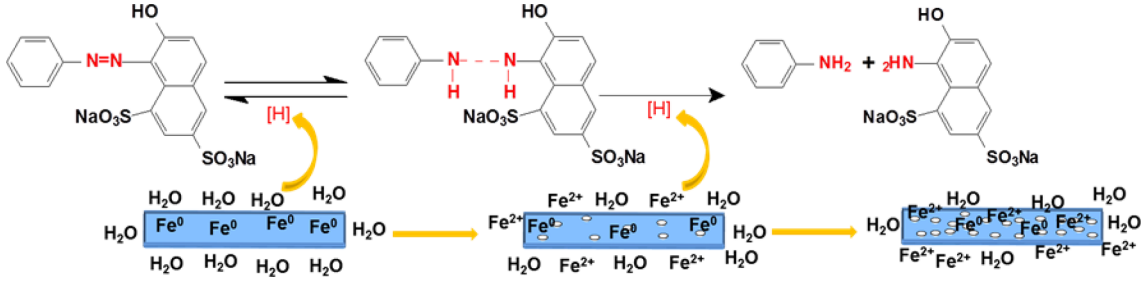

affirmed another virtue that it can be easily taken out from the solution and the sediments by a small external magnetic field.

DISCUSSION

According to XRD spectra, the shift of 2θ towards a low angle was found in $Fe_{66.3}B_{16.6}Y_{17.1}$, similar to that of $Fe_{11}Y_3$. It is obvious that the primary bonding associated with strong Fe−B in Fe_8B_2 was not dominant in $Fe_{66.3}B_{16.6}Y_{17.1}$. In XPS spectra, the strong Fe−B hybridization is characterized by the peak at 8.7 eV in $Fe_{79}B_{16}Si_5$ but that does not exist in $Fe_{66.3}B_{16.6}Y_{17.1}$. The detected peak of $Fe_{66.3}B_{16.6}Y_{17.1}$ was shifted to 10.6 eV, about 1.9 eV away from the peak corresponding to Fe−B hybridization and close to the peak of B-2p electron. The occurrence of the shoulder is a consequence of a majority- and minority-spin electron band system, separated by the exchange splitting.[22,27] The absence of the shoulder indicated the small splitting between the majority and minority, and thus more Fe electrons are paired. Compared with these ZVIs, the ZVI with more unpaired electrons should be more active, as evidenced by the fresh iron[3,4] and the $Fe_{66.3}B_{16.6}Y_{17.1}$ studied here. The 3d electron distribution of ZVI in $Fe_{66.3}B_{16.6}Y_{17.1}$ is similar to pure iron, which indicates the interaction between Fe−Y is also weak. Compared with Fe_8B_2 and $Fe_{11}Y_3$, the introduction of $Fe_{11}Y_3$ into an Fe_8B_2 cluster constructs a metastable atomic arrangement to dilute the interaction between Fe and its neighbor atoms, and, as a result, the ZVI could be seen as a "pseudo-isolated" iron, "frozen" in $Fe_{66.3}B_{16.6}Y_{17.1}$.

During the decolorization process, the ZVI was oxidized to generate free electrons while the "-N═N-" bond acted as an acceptor and broke into two amino groups ($-NH_2$) that locate at their local moiety, respectively[3,6,28,29] (Scheme 1). In other words, the OG was split to aniline and 1-amino-2-naphthol-6,8-disulfonic acid salt.[30] The released Fe^{2+}/Fe^{3+} in water is 0.0866 mg/L after 180 min for $Fe_{66.3}B_{16.6}Y_{17.1}$ (Table S1), which means the deterioration of water quality is ignorable.[31] Compared with 77 mg/L Fe^{2+}/Fe^{3+} released into water after decolorization of Azo dye by Fe−Si−B−Mo,[25] $Fe_{66.3}B_{16.6}Y_{17.1}$ is substantially more eco-friendly. The B was also detected in the filtrate, but it does not contribute to the decolorization (Figure S3). In order to make a contrast, the pure B powders were stirred with water and OG solution respectively for a fixed duration. As the results, the B concentration of the two filtrates is equivalent (Table S2). No Y ion was detected in the filtrate, so it does not take part in the decolorization. During the reaction, it was

dx.doi.org/10.1021/am501014s | ACS Appl. Mater. Interfaces 2014, 6, 5500−5505

peeled from the foil and then enclosed in the sediments (Table S1). The calculated decolorization efficiency of $Fe_{66.3}B_{16.6}Y_{17.1}$ is 99.7%. It is much higher than other samples (Table S3). The iron powder is low cost but easy to be oxidized, thus it needs low pH value and inert gas protection during the reaction. It is also difficult to reuse.[3] The $Fe_{11}Y_3$ has a strong interaction between Fe-d and Y-d states like the Fe−B interaction in $Fe_{79}B_{16}Si_5$[32,33] and reported $Fe_{78}B_{14}Si_8$[7] (Figure S4). With this strong interaction, the ZVI inside them showed equivalent performances in decolorization, which were much inferior to that of $Fe_{66.3}B_{16.6}Y_{17.1}$. The k value of $Fe_{79}B_{16}$ Si_5 from Figure 5b is 0.0044 min^{-1}, and the calculated $t_{1/2}$ is 160 min. This value is well consistent with the decolorization efficiency of 51.5% after 180 min. The decolorization kinetics plot of $Fe_{66.3}B_{16.6}Y_{17.1}$ (Figure 5a) exhibits two stages with k values of 0.011 min^{-1} and 0.047 min^{-1}, respectively. Moreover, the observed $t_{1/2}$ is 64 min, which is in good accordance with the calculated value 63 min. However, if k_1 (0.011 min^{-1}) dominated the total decolorization process, the expected reaction time of 407 min (4.48/0.011, 4.48 is highlighted in Figure 5a) will be much longer than the observed 180 min. This means the existence of the second, accelerated stage with k_2 = 0.047 min^{-1} and highlights its contribution to the fast decolorization. After the first 180 min, the cyclic decolorization experiments were carried out by refreshing the same OG solution in order to verify the change of the k value. The reaction time was expected to decrease to approximately 95 min, which was calculated via 4.48/0.047. The UV-vis spectra are measured after 95 min for cycle2 and cycle3.[34] The detected absorption values equaled to the one after the first cycle (Figure 8). These evidences

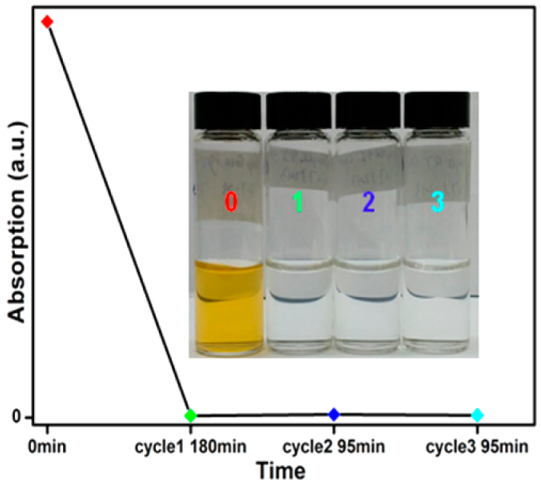

Figure 8. Absorption of treated solution in 3 decolorization cycles.

reconfirmed the value of the rate constant of the second stage k_2, and that the two stages of reaction well represented the course of decolorization. The longtime cyclic test shows the fast decolorization was conducted up to the 11th cycles (Figure S5).

From SEM examination, only the surface of $Fe_{66.3}B_{16.6}Y_{17.1}$ had obvious pits. According to the mapping of a selected hole giving in Figure 7, the ZVI was enriched at the bottom of the holes. In Figure S6, the change of $Fe_{66.3}$ $B_{16.6}Y_{17.1}$ was monitored with time, and only several small holes were found within the initial 45 min. The Fe/Y (at %) at the bottom of the hole was increased to 8.86, while the raw material had an average Fe/Y ratio of 3.86 (Table S1). After 90 min, the holes distribution was similar to that after 180 min and Fe/Y changed to 29.03, which was close to the value of 26.10 after 180 min. At the same time, the Fe/Y ratio on the flat surface of $Fe_{66.3}B_{16.6}Y_{17.1}$ remained at 3.52, and the change could be neglected. The ZVI at the surface was separated from the destabilized Fe−B−Y atomic arrangement continuously and vacancies formed. With more vacancies, the free energy of Fe−B−Y in the vicinity gradually increased and the atomic arrangement became less stable. During this process, the ZVI carrying extra free energy contributed to the fast decolorization not only as a reducing agent but also a catalyst. Furthermore, this can also explain the observed transition from slow to fast kinetics corresponding to the change from k_1 to k_2. In summary, the competitive effect between two types of clusters not only helped to provide ZVI with high activity but also brought a catalytic effect to assist the reduction of the "-N═N-"bond. The short reaction time and well reusability make it a potential candidate to replace traditional physical, chemical, and biological treatments, and the resulting aromatic amine could be used to fertilize microorganisms and become nontoxic.[17] Herein, we provide a feasible strategy to fabricate new highly active metal materials for converting toxic material to much less harmful species and highlight the advantages.

CONCLUSION

In conclusion, the novel Fe-rich amorphous structure with the composition of $Fe_{66.3}B_{16.6}Y_{17.1}$ was designed from the competitive cluster principle. The model decolorization is totally finished within 180 min in the first cycle and then changes to 95 min spontaneously during the consumption of ZVI until the 11th cycles. Compared with iron powder, $Fe_{79}B_{16}Si_5$, and $Fe_{11}Y_3$, the new ZVI has advantages as follows: I) the designed atomic arrangement allows the high active ZVI to hold in II) the energy released during the separation of ZVI from the Fe−B−Y arrangement and can catalyze the decolorization; III) the small amount of the constituent element is consumed, and no secondary hazard in water is generated; IV) at last, the rapid decolorization was carried out at moderate conditions, and the ZVI has good reusability. This work demonstrates the significance of tuning the atomic arrangement in the designing of highly active metal materials and reports for the first time the catalysis effect origins from the destabilized atomic arrangement. It also indicates a brilliant future of using highly active metal materials to treat environmental pollutants practically.

ASSOCIATED CONTENT

Supporting Information

The morphology of $Fe_{79}B_{16}Si_5$, $Fe_{11}Y_3$. and $Fe_{66.3}B_{16.6}Y_{17.1}$ after 180 min decolorization (Figure S1), the room temperature magnetization curve of $Fe_{66.3}B_{16.6}Y_{17.1}$ after decolorization (Figure S2), the OG treated by the pure B (Figure S3), the OG treated by the reported $Fe_{78}B_{14}Si_8$ (Figure S4), the longtime cyclic decolorization (Figure S5), the atom ratio change of Fe and Y and the morphology of $Fe_{66.3}B_{16.6}Y_{17.1}$ surface with reaction time (Figure S6), the trace of elements before and after reaction (Table S1), the ICP tests of various samples for comparison (Table S2), the decolorization efficiency of other samples (Table S3). This material is available free of charge via the Internet at http://pubs.acs.org.

AUTHOR INFORMATION

Corresponding Authors

*E-mail: pengliu198354@gmail.com (P.L.).

*E-mail: apchshek@cityu.edu.hk (C.H.S.).

Notes

The authors declare no competing financial interest.

■ ACKNOWLEDGMENTS

The work described in this paper was fully supported by a grant from the Research Grants Council of the Hong Kong Special Administrative Region, China [Project No. (RGC Ref. No.), CityU 119212].

■ REFERENCES

(1) Agrawal, A.; Tratnyek, P. G. Reduction of Nitro Aromatic Compounds by Zero-Valent Iron Metal. *Environ. Sci. Technol.* **1996**, *30*, 153−160.
(2) Eykholt, G. R.; Davenport, D. T. Dechlorination of the Chloroacetanilide Herbicides Alachlor and Metolachlor by Iron Metal. *Environ. Sci. Technol.* **1998**, *32*, 1482−1487.
(3) Jiasheng, C.; Liping, W.; Qingguo, H.; Lian sheng, W.; Shuokui, H. Reducing Degradation of Azo Dye by Zero-Valent Iron in Aqueous Solution. *Chemosphere* **1999**, *38*, 565−571.
(4) Sangkil, N.; Trantnyek, P. G. Reduction of Azo Dyes with Zero-Valent Iron. *Water Res.* **2000**, *34*, 1837−1845.
(5) Abazari, R.; Heshmatpour, F.; Balalaie, S. Pt/Pd/Fe Trimetallic Nanoparticle Produced via Reverse Micelle Technique: Synthesis, Characterization, and Its Use as an Efficient Catalyst for Reductive Hydrodehalogenation of Aryl and Aliphatic Halides under Mild Conditions. *ACS Catal.* **2013**, *3*, 139−149.
(6) Wang, J.-Q.; Liu, Y.-H.; Chen, M.-W.; Xie, G.-Q.; Louzguine-Luzgin, D. V.; Inoue, A.; Perepezko, J. H. Rapid Degradation of Azo Dye by Fe-Based Metallic Glass Powder. *Adv. Funct. Mater.* **2012**, *22*, 2567−2570.
(7) Zhang, C.; Zhu, Z.; Zhang, H.; Hu, Z. Rapid Decolorization of Acid Orange II Aqueous Solution by Amorphous Zero-Valent Iron. *J. Environ. Sci.* **2012**, *24*, 1021−1026.
(8) Liang Zhang, J.; Min Wang, Y.; Hung Shek, C. Design of Soft Magnetic CoSiB Metallic Glass with Low Co Contents. *J. Appl. Phys. (Melville, NY, U. S.)* **2011**, *110*, 083919.
(9) Dong, C.; Wang, Q.; Qiang, J. B.; Wang, Y. M.; Jiang, N.; Han, G.; Li, Y. H.; Wu, J.; Xia, J. H. From Clusters to Phase Diagrams: Composition Rules of Quasicrystals and Bulk Metallic Glasses. *J. Phys. D: Appl. Phys.* **2007**, *40*, R273−R291.
(10) Miracle, D. B. A Structural Model for Metallic Glasses. *Nat. Mater.* **2004**, *3*, 697−702.
(11) Chien, C. Mössbauer Study of a Binary Amorphous Ferromagnet: $Fe_{80}B_{20}$. *Phys. Rev. B: Condens. Matter Mater. Phys.* **1978**, *18*, 1003−1015.
(12) den Broeder, F. J. A.; van der Borst, J. $Fe_{80}B_{20-x}Si_x$ Glasses: A Study of Some Physical Properties as Depending on Metalloid Content. *J. Appl. Phys. (Melville, NY, U. S.)* **1979**, *50*, 4279.
(13) Zhang, J.; Tan, H.; Feng, Y. P.; Li, Y. The Effect of Y on Glass Forming Ability. *Scr. Mater.* **2005**, *53*, 183−187.
(14) Zhang, W.; Liu, G.; Han, K. The Fe-Y (Iron-Yttrium) System. *J. Phase Equilib.* **1992**, *13*, 304−308.
(15) Miracle, D. B.; Wilks, G. B.; Dahlman, A. G.; Dahlman, J. E. The Strength of Chemical Bonds in Solids and Liquids. *Acta Mater.* **2011**, *59*, 7840−7854.
(16) Bokare, A. D.; Chikate, R. C.; Rode, C. V.; Paknikar, K. M. Iron-Nickel Bimetallic Nanoparticles for Reductive Degradation of Azo Dye Orange G in Aqueous Solution. *Appl. Catal. B* **2008**, *79*, 270−278.
(17) Kolekar, Y. M.; Pawar, S. P.; Gawai, K. R.; Lokhande, P. D.; Shouche, Y. S.; Kodam, K. M. Decolorization and Degradation of Disperse Blue 79 and Acid Orange 10, by Bacillus Fusiformis KMK5 Isolated from The Textile Dye Contaminated Soil. *Bioresour. Technol.* **2008**, *99*, 8999−9003.
(18) Xu, X.-R.; Li, X.-Z. Degradation of Azo Dye Orange G in Aqueous Solutions by Persulfate with Ferrous Ion. *Sep. Purif. Technol.* **2010**, *72*, 105−111.
(19) Zhu, C. L.; Wang, Q.; Li, F. W.; Li, Y. H.; Wang, Y. M.; Dong, C.; Zhang, W.; Inoue, A. Cluster-Based Bulk Metallic Glass Formation in Fe-Si-B-Nb Alloy Systems. *J. Phys.: Conf. Ser.* **2009**, *144*, 012048.
(20) Matsuura, M.; Nomoto, T.; Itoh, F.; Suzuki, K. Xps Study of The Valence Band Spectrum of Amorphous Fe-B Alloys. *Solid State Commun.* **1980**, *33*, 895−897.
(21) Hafner, J.; Tegze, M.; Becker, C. Amorphous Magnetism in Fe-B Alloys: First-Principles Spin-Polarized Electronic-Structure Calculations. *Phys. Rev. B: Condens. Matter Mater. Phys.* **1994**, *49*, 285−298.
(22) Joyner, D.; Johnson, O.; Hercules, D.; Bullett, D.; Weaver, J. Study of the Iron Borides. IV. Relation of Bonding to Structure and Magnetic Behavior from Photoemission Experiments and ab Initio Calculations. *J. Phys. Rev. B: Condens. Matter Mater. Phys.* **1981**, *24*, 3122−3137.
(23) Joyner, D. J.; Johnson, O.; Hercules, D. M. A Study of The Iron Borides. 1. Electron-spectroscopy. *J. Am. Chem. Soc.* **1980**, *102*, 1910−1917.
(24) Connell, G. A. N.; Oh, S.-J.; Allen, J.; Allen, R. The Electronic Density of States of Amorphous Y-Fe and Tb-Fe Alloys. *J. Non-Cryst. Solids* **1984**, *61&62*, 1061−1066.
(25) Zhang, C.; Zhang, H.; Lv, M.; Hu, Z. Decolorization of Azo Dye Solution by Fe−Mo−Si−B Amorphous Alloy. *J. Non-Cryst. Solids* **2010**, *356*, 1703−1706.
(26) King, G. A.; Oliver, T. A.; Ashfold, M. N. Dynamical Insights into $^1\pi\sigma^*$ State Mediated Photodissociation of Aniline. *J. Chem. Phys.* **2010**, *132*, 214307.
(27) Paul, T.; Neddermeyer, H. Experimental Investigation of The Electronic Structure of Amorphous and Crystalline Fe_xB_{100-X} ($75 \leq x \leq 87$). *J. Phys. F: Met. Phys.* **1985**, *15*, 79−89.
(28) Reza, S. M.; Mansur, Z.; Abdeltif, A.; Noori, S. M.; Mehdi, N.; Saied, N.; Ahmad, Z. Kinetic of Degradation of Two Azo Dyes from Aqueous Solutions by Zero Iron Powder: Determination of The Optimal Conditions. *Desalin. Water Treat.* **2012**, *40*, 137−143.
(29) Shirin, S.; Balakrishnan, V. K. Using Chemical Reactivity to Provide Insights Into Environmental Transformations of Priority Organic Substances: The Fe^0-mediated Reduction of Acid Blue 129. *Environ. Sci. Technol.* **2011**, *45*, 10369−77.
(30) Muthukumar, M.; Karuppiah, M. T.; Raju, G. B. Electrochemical Removal of CI Acid Orange 10 from Aqueous Solutions. *Sep. Purif. Technol.* **2007**, *55*, 198−205.
(31) Li, T.; Chen, Y.; Wan, P.; Fan, M.; Yang, X. J. Chemical Degradation of Drinking Water Disinfection Byproducts by Millimeter-Sized Particles of Iron−Silicon and Magnesium−Aluminium Alloys. *J. Am. Chem. Soc.* **2010**, *132*, 2500−2501.
(32) Becker, C.; Hafner, J. Structural, Electronic, and Magnetic Properties of Fe-Y Alloys. *J. Phys. Rev. B: Condens. Matter Mater. Phys.* **1994**, *50*, 3913−3930.
(33) Vincze, I.; Boudreaux, D. S.; Tegze, M. Short-Range Order in Fe-B Metallic Glass Alloys. *Phys. Rev. B: Condens. Matter Mater. Phys.* **1979**, *19*, 4896−4900.
(34) In the cyclic decolorization test, we observed the change of OG solution with time by vision. The yellow color of the solution nearly disappears after 95 min, and the appearance of the solution is similar to the one after the first cycle. After that, about 1 mL of solution was filtrated to measure the absorption for cycle2 and cycle3.